Acta Cryst. (1996). D**52**, 799–805

Interconversion of Crystals of the *Escherichia coli* EF-Tu·EF-Ts Complex Between High- and Low-Diffraction Forms

TAKEMASA KAWASHIMA,* CARMEN BERTHET-COLOMINAS, STEPHEN CUSACK AND REUBEN LEBERMAN

EMBL Grenoble Outstation, BP 156, 38042 Grenoble CEDEX, France. E-mail: tax@embl-grenoble.fr

(*Received 27 September 1995; accepted 13 February 1996*)

Abstract

Crystals of the complex formed between the two bacterial polypeptide elongation factors, EF-Tu and EF-Ts, produced from solutions of PEG 6000 can be of two morphologically similar forms both of space group $P2_12_12_1$. One form diffracts to only about 3 Å resolution, the other to better than 2.4 Å resolution. These forms can be interconverted and the transformation of one into the other has been shown to be solely a result of dehydration/hydration processes. By designing a suitable soaking protocol and careful control of the experimental parameters for data collection at cryo-temperatures, complete data sets for the high-resolution form could be obtained.

1. Introduction

The bacterial polypeptide elongation factor Tu (EF-Tu) has the central role in protein biosynthesis of transporting charged elongator tRNA's to the active mRNA:ribosome complex. It is a representative of the large family of G proteins involved in the regulation of a wide range of metabolic processes [see Bourne, Sanders & McCormick (1990, 1991) for reviews]. These proteins share a common reaction scheme which requires the binding and the hydrolysis of guanosine 5′-triphosphate (GTP) to guanosine 5′-diphosphate (GDP) in switching from the active to inactive states. The replacement of the tightly bound GDP by GTP to produce the active protein is ensured by a protein called the guanine nucleotide exchange factor, which in the case of EF-Tu is elongation factor Ts (EF-Ts). In order to investigate the molecular mechanism by which EF-Ts releases the guanine nucleotide, the complex of the two elongation factors have been isolated and crystallized for X-ray diffraction studies. Although this complex was crystallized more than a decade ago (Leberman, Schulz & Suck, 1981; Schneider, 1983) the structure was only recently solved to high resolution (Kawashima, Berthet-Colominas, Wulff, Cusack & Leberman, 1996). The previous report suggested that crystals of the complex obtained from PEG 6000 solutions could exist in two interchangeable forms both with the space group $P2_12_12_1$; one with cell parameters $a = 81.7$, $b = 110.5$, $c = 206.0$ Å and diffracting to 4.5 Å on a rotating-anode X-ray generator, and the other with cell parameters $a = 74.3$, $b = 108.7$, $c = 198.5$ Å and a diffraction limit beyond 3 Å, as measured on films. Since the high-resolution form was originally found when trying to produce a methyl mercury acetate derivative by soaking crystals of the low-resolution form, the change in the cell parameters and the diffraction limit was, at that time, attributed to the binding of heavy-metal compound. We describe here the crystallization conditions and the techniques required to overcome the problems of crystal transformation which was the major barrier to consistent data collection. While this study was underway, a report was published (Schick & Jurnak, 1994) on the extension of the diffraction resolution of EF-Tu·EF-Ts crystals grown from PEG 4000 solutions by gradually changing the solvent to higher concentrations of higher molecular weight fractions of PEG.

2. Materials and methods

2.1. *EF-Tu·EF-Ts*

The majority of crystals used were of samples of EF-Tu·EF-Ts isolated from *Escherichia coli* (N4830-1, Pharmacia) transformed with the expression vector pCP40 (Remaut, Tsao & Fiers, 1983) habouring the EF-Ts gene, following previously described protocols (Leberman *et al.*, 1980; Wittinghofer, Guariguata & Leberman, 1983) but using buffers without added Mg^{2+}. Assays for EF-Tu and EF-Ts were made by standard filter binding procedure and [^{3}H]GDP exchange (Wittinghofer & Leberman, 1976). Polyacrylamide gel electrophoresis in the presence of sodium dodecyl sulfate was carried out in a continuous buffer system of Tris–bicine (Ziegler, Harrison & Leberman, 1974).

2.2. *Crystallization*

Crystallization screening was carried out by vapour diffusion using the hanging-drop method whereas optimizing of conditions was carried out using the

sitting-drop method. The reproducible final conditions were: 40 µl drops containing 2.5 mg ml^{-1} EF-Tu·EF-Ts complex, 10% PEG 6000 (Fluka), 100 m*M* KCl, Tris–HCl (64.4 m*M* Tris), pH 7.7, equilibrated against 2 ml solution containing all components except no protein, and 20% PEG 6000, at ambient temperature (292–298 K).

2.3. *Data collection*

Crystals were mounted in glass capillaries and sealed while still containing a microdrop of mother liquor. The X-ray diffraction measurements were made with a Rigaku RU200 BH rotating-anode X-ray generator operating at 100 mA and 40 kV

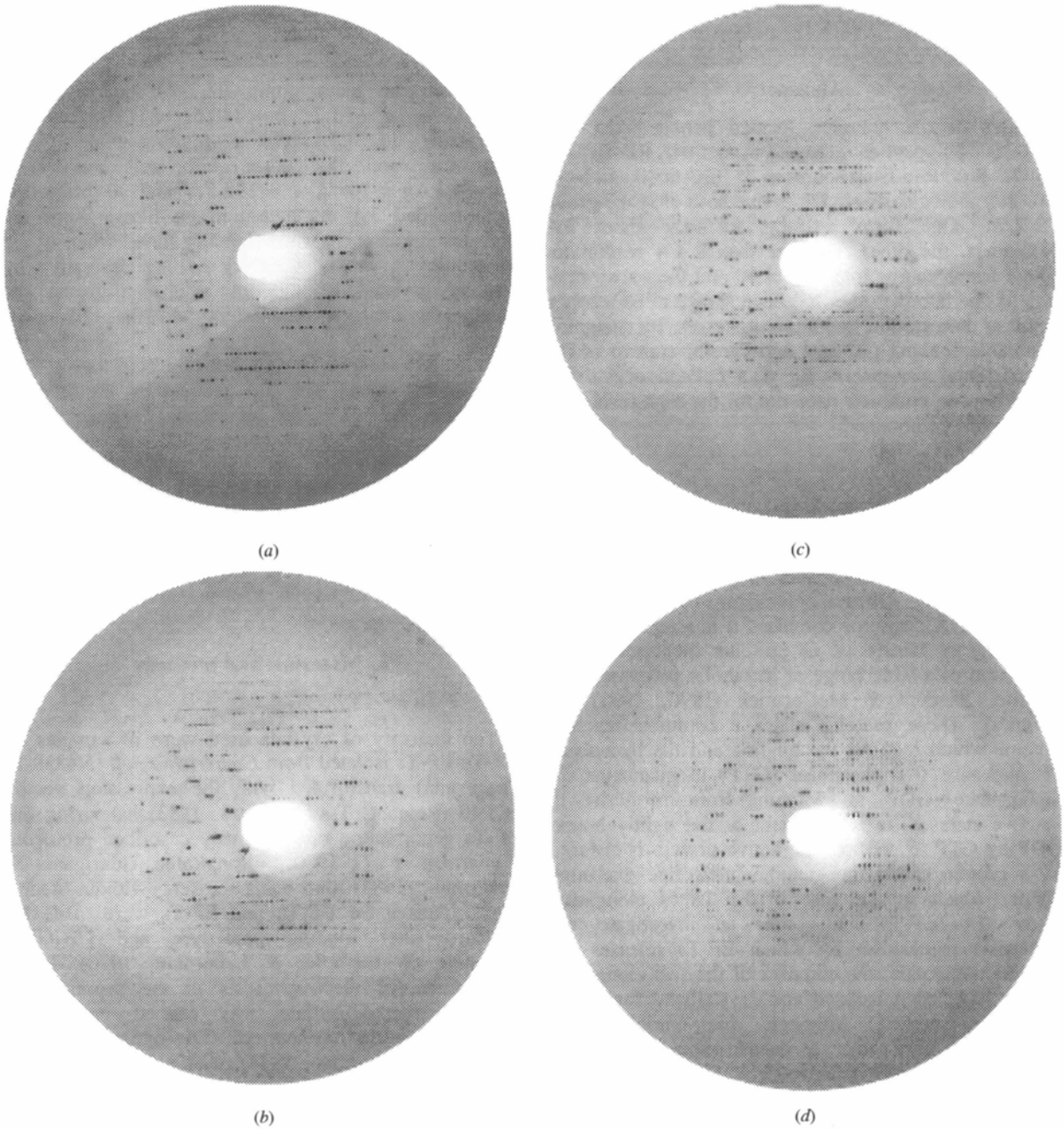

Fig. 1. Sequential frames in an X-ray diffraction data collection of a low-diffraction form of an EF-Tu·EF-Ts crystal soaked in 100 m*M* ethyl mercury chloride. (*a*) Initial diffraction pattern. The approximate orientation is *c* axis parallel to the oscillation axis (horizontal), *a* axis vertical, and *b* axis parallel to the X-rays. (*b*) after 3.5 h irradiation; (*c*) after 4.5 h irradiation; (*d*) after 6.5 h irradiation.

($\lambda = 1.54$ Å), with double-mirror focusing and monochromatic optics, the size of the beam being 300×300 μm after the slits. The detector used was a commercial 150 mm MAR Research on-line image-plate system. The crystal was mounted and oriented to have the *c* axis as parallel as possible to the spindle axis. The data collection started with the *b* axis almost parallel to the X-rays. The set up was a 2° oscillation range for 30 min exposure time and six oscillations per frame, at a crystal-to-detector distance of 220 mm, which sets the outer limit of the detector at 4 Å resolution. The cooling air stream was coaxial to the spindle axis. The crystal was soaked for 1.5 h in a solution containing 100 μ*M* ethylmercury chloride, 23%(*w*/*v*) PEG 6000, 80 m*M* KNO_3, buffered at pH 7.7 with Tris–acetate (64.4 m*M* Tris).

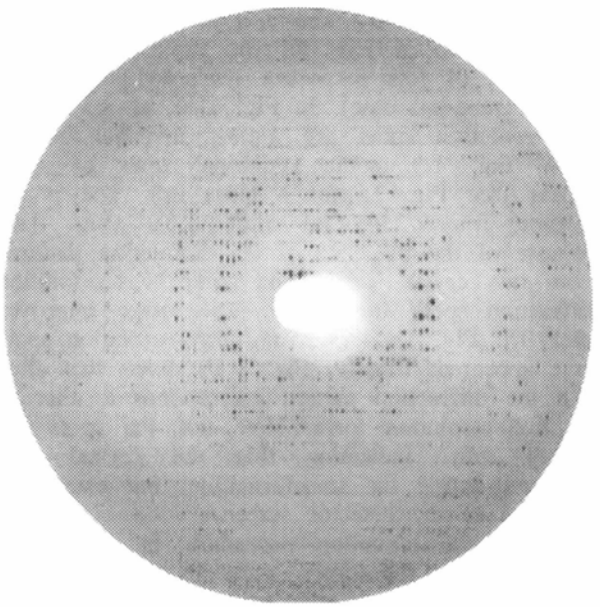

(*e*)

(*f*)

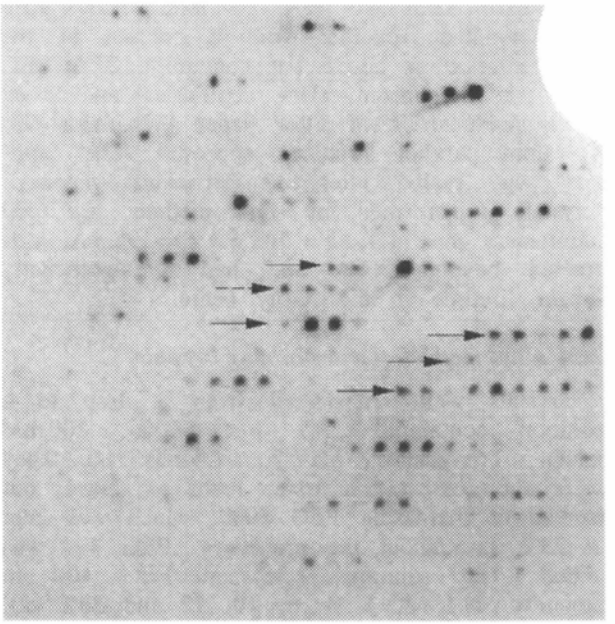

(*g*)

Fig. 1 (*cont.*) Diffraction pattern (*e*) after 9 h irradiation; (*f*) after 11 h irradiation. The value of φ, the angle about the rotation axis, is the same as in (*a*). (*g*) Close-up view of a region in the bottom-left quadrant of the image (*c*). Two examples are shown, thick arrows pointing to diffraction spots initially present, and dotted arrows pointing to newly appeared rows of spots.

2.4. *Initial method of transforming crystals*

Crystals were transferred from a drop to a solution containing 23% PEG 6000, 100 m*M* KCL, 64.4 m*M* Tris–HCl, pH 7.7, or 23% PEG 6000, 100 m*M* KNO_3 and Tris–acetate (64.4 m*M* Tris) pH 7.7. They were subsequently passed through solutions of the same salts containing increasing amounts of PEG 6000, from 23 to 26%, in steps of 0.5%, the soaking time in each bath being at least 15 min. They were then mounted, together with a column of the same solution as above but containing 27% PEG 6000, in siliconized glass capillaries and dried gently with strips of filter paper (Whatman No. 4), until parallel striations appeared. The capillary was sealed after the striations vanished. Crystals transformed by this method had cell parameters $a = 74.5$, $b = 109.6$, $c = 198.8$ Å, diffracted beyond 2.4 Å and had a significantly longer lifetime in the X-ray beam.

2.5. *Final method of transforming crystals*

Crystals were transferred from a drop to a solution containing 23% PEG 6000, 100 m*M* KNO_3, Tris–acetate (pH 7.7, 64.4 m*M* Tris). They were subjected to successive baths as above, but instead of increasing PEG 6000, which was kept at 23% throughout the procedure, PEG 400 was added. The solutions contained PEG 400 in amounts of 1, 2, 3, 4, 5, 10, 15 and 20%, all other components being the same, as well as the soaking time. This transformation procedure was adopted for the data collection on high-resolution crystals at 110 K.

3. Results and discussion

Under the crystallization conditions described above, crystals appeared after about two weeks and were left to grow for at least one month, when they reached an average size of $400 \times 300 \times 200$ µm. They had the same morphology as those previously reported (Leberman *et al.*, 1981; Schneider, 1983) and belonged to space group $P2_12_12_1$, with cell dimensions $a = 80.3$, $b = 109.5$, $c = 204.6$ Å, slightly different from those described. They diffracted weakly to 3 Å as measured on an image plate with a conventional X-ray generator, and were very sensitive to radiation.

The previous report (Leberman *et al.*, 1981), indicated the possibility of transforming the low-resolution form to the high-resolution form by binding heavy-metal compounds although it was not clear whether one form derived from the other or the two forms coexisted in the same drop. The observation that clearly demonstrated that the high-resolution form could be derived from the low-resolution form is presented in Fig. 1. This shows a sequence of frames taken during an attempt to collect a derivative data set (details in *Materials and methods*) and strikingly illustrates the change in diffraction patterns as the low-resolution form tranformed into the high-resolution form during the data-collection procedure. Fig. 1(*a*) shows the initial diffraction image of the low-resolution form. The following frames show the diffraction patterns for the same crystal with the times of total exposure (*i.e.* do not include scanner read-out time). In Fig. 1(*b*), at 3.5 h, the high-resolution spots are almost invisible but at 4.5 h (Fig. 1*c*), some additional rows of spots appear (see Fig. 1*g* for a close up). The image becomes more confused after 6.5 h (Fig. 1*d*), because of the presence of the diffraction patterns from two crystal forms and some high-resolution diffraction spots are visible. The image improves after 9 h (Fig. 1*e*) and strong high-resolution spots have appeared. Finally, Fig. 1(*f*) shows that after 11 h the diffraction pattern corresponds to that of the high-resolution form. Note that the spots are mostly split, indicating that the crystal was damaged during the transformation, but extend to the edge of the detector screen.

During the mounting procedure in capillaries, crystals were sometimes accidentally dried 'too hard' and showed parallel striations perpendicular to the *a* axis. These crystals would still diffract to high resolution, although the data were not usable because of the split spots of the diffraction patterns. In addition, with cooling, droplets were observed, slowly migrating from the mother liquor in the capillary, because of the presence of a temperature gradient. These observations led to the conclusion that the high-resolution form was derived from the low-resolution form by distillation of water from the crystal because of the diffraction experiment set-up and that transformation into the high-resolution form could be achieved by controlled dehydration.

Although the transformation by the initial procedure could be performed reasonably well under home laboratory conditions, the stability of the dehydrated form strongly depended on the temperature and humidity of the working environment. Measurements of crystals mounted in an environment where temperature and humidity were not well controlled were often unsatisfactory because of the reconversion of crystals back to the low-resolution form. The geometry of the cooling system, *i.e.* how the crystal and the liquid (mother liquor) column are exposed to the cooled air-stream, could generate a temperature

gradient which might also contribute to this back transformation. In addition, it was thought preferable that screening for heavy-atom derivatives should be performed with the crystals already transformed in order to minimize the potential isomorphous difference introduced by the

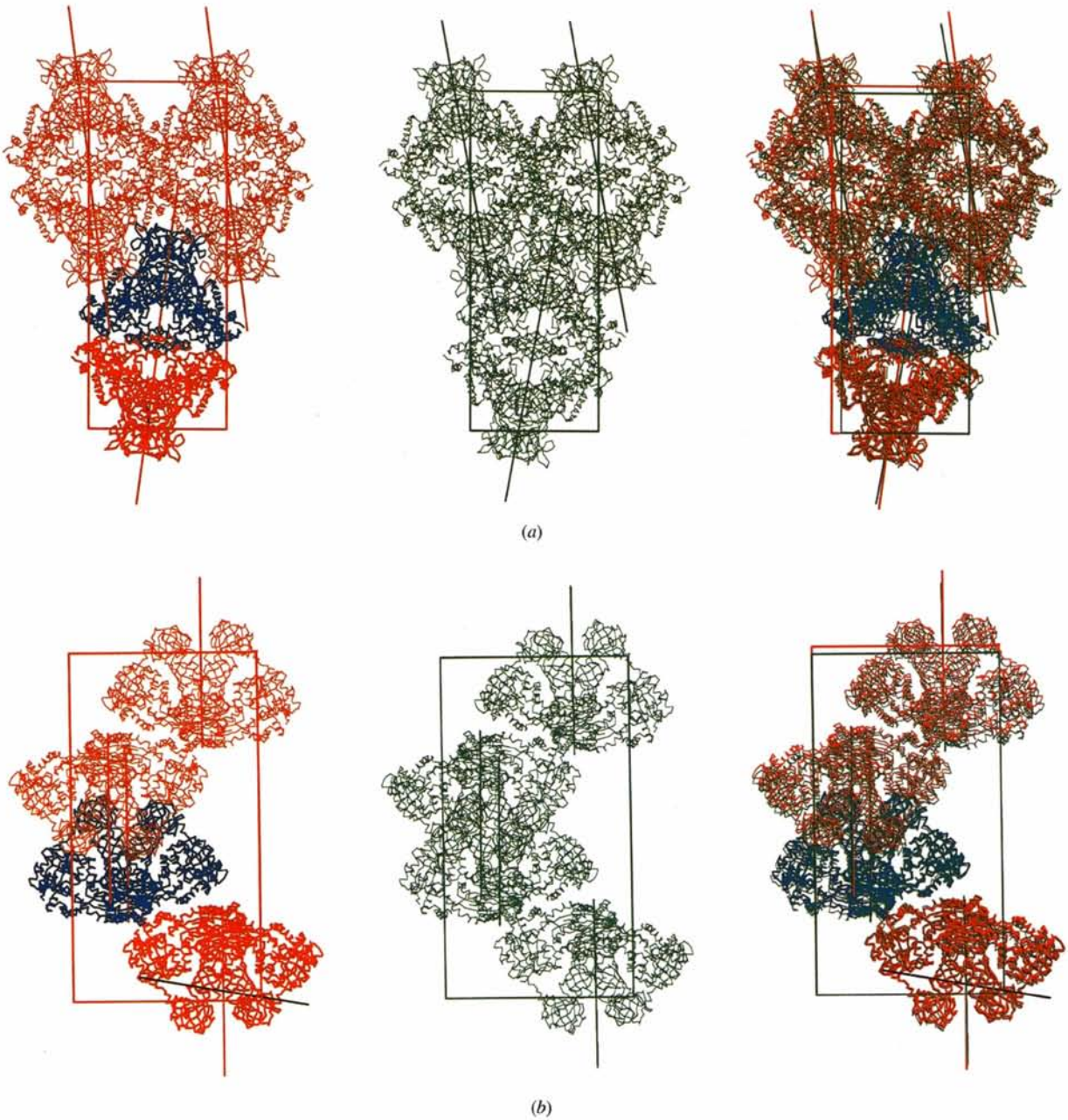

Fig. 2. Overall view of the change in crystal packing between the low- and high-resolution forms. The Cα trace of the molecules, their associated non-crystallographic pseudo-twofold axes and the unit cell are in red for the low-resolution form and green for the high-resolution form. A pair of dimers, referred to as 'the moving unit', is in thick lines, one dimer is in blue. As an example, the rotation axis about which the moving unit must turn to be superimposed on the corresponding dimers in the high resolution form is represented by a black line. The figures from left to right are: the low-resolution form, the high-resolution form, the superposition of both forms by their respective crystallographic origins. (*a*) Viewed down the *b* axis, with the *a* axis horizontal and the *c* axis vertical, showing the effect of the molecular movements on the cell parameters *a* and *c*. Note that the rotation axis, being almost perpendicular to the plane of the figure, is hardly visible. (*b*) Viewed 90° rotated from (*a*) *i.e.* down the *a* axis, with the *b* axis horizontal and the *c* axis vertical, showing that the non-crystallographic pseudo-twofold axis is parallel to the (*a*,*c*) plane. There is barely any effect on the cell parameter *b*. See text for explanations. Figures produced with *MOLSCRIPT* (Kraulis, 1991).

transformation process in addition to the one from the heavy atoms themselves.

The above considerations led to the design of the second protocol to be used with crystals destined for data collection at 110 K. This gave highly reproducible results, provided PEG solutions were fresh, *i.e.* every crystal subjected to this protocol reannealed and macroscopically showed no damage. It is the tuning of this protocol that became a crucial step in solving the high-resolution structure. The crystals produced by this procedure diffracted beyond 2.4 Å, had cell dimensions of $a = 73.53$, $b = 108.54$ and $c = 194.55$ Å at 100 K and were used for the final 2.5 Å structure determination.

Our observations extend those described by Schick & Jurnak (1994) on the same crystal system. They attributed the extension of the diffraction resolution as being because of the diffusion of the higher molecular weight PEG's, into the crystals with a concomitant reduction in solvent content. However, all our observations are consistent with the two crystal forms of EF-Tu·EF-Ts being solely dependent of their degree of hydration, and that the transformation observed in the course of the data collection (Fig. 1) is caused by bulk movement of water. This has the effect of increasing (decreasing) the concentration of PEG 6000 in the mother liquor and consequently dehydrating (rehydrating) the crystal itself in a process more akin to dialysis. We have also shown that the transformation can occur under controlled conditions in bulk solvent, either by gradually increasing the concentration of PEG 6000, or at constant PEG 6000 concentration and gradually addition of PEG 400. The latter procedure is preferable since PEG 400 is a good cryo-protectant, and data collection on highly diffracting transformed crystals at 110 K might also help prevent rehydration.

A similar case was reported in another system, where crystals of HIV-1 reverse transcriptase belonging also to space group $P2_12_12_1$ were obtained by equilibration of a sitting drop against a reservoir containing 6% PEG 3400. A further equilibration with 46% PEG 3400 solution over 3 d could be performed to slowly dehydrate the crystals and improve diffraction power, accompanied by a decrease in solvent content of as much as 25% (Stammers *et al.*, 1994; Esnouf *et al.*, 1995). As a comparison, the decrease in solvent content in the case of EF-Tu·EF-Ts crystals is 5%.

Having now solved and refined the crystal structure of the highly diffracting form of the EF-Tu·EF-Ts complex at cryo-temperatures to 2.5 Å resolution (Kawashima *et al.*, 1995), we are now in a position to examine the molecular rearrangements accompanying the crystal transformation in more detail. Using a 3.5 Å data set for the low-diffracting form and a 3 Å data set for the high-diffracting form, both measured at room temperature, we have solved the structures of both forms using *AMoRe* (Navaza, 1994) for molecular replacement and *X-PLOR* (Brünger, 1992) for subsequent rigid-body refinement. Although the quality of the data does not permit a detailed model refinement and examination of the crystal contacts, the following conclusions can be made.

The asymmetric unit of the EF-Tu·EF-Ts complex crystals can be considered as a dimer of two complexes, this we designate as $[EF\text{-}Ts]_2 \cdot 2EF\text{-}Tu$ since EF-Ts forms intimate homodimer contacts whereas each EF-Tu binds principally to one EF-Ts. The non-crystallographic pseudo-twofold axis relating the two complexes is almost parallel to the crystal *c* axis, tilted by approximately 10° with respect to the latter, in a plane perpendicular to the *b* axis. In both high- and low-resolution room-temperature structures, this tilt angle is reduced. In order to superimpose the room-temperature low-resolution structure on the room-temperature high-resolution structure, a rotation of 4° about an axis 15° apart from the *b* axis is required (Fig. 2). This might explain the minor change observed in the parameter *b* as compared to the change for *a* and *c*, or that the crystal was macroscopically twisted along the *b* axis (see extended discussion in deposited materials). In fact, it is not only each dimer but a pair of dimers related by crystallographic symmetry that moves as a rigid body between the two forms, such that at least one crystal contact is preserved. It is clear from this preliminary result, that there are, indeed, two distinct crystal forms with slightly different packings. The investigation of the precise change in crystal contacts, however, would require structure determination of both forms, at higher resolution.*

We would like to thank Dr O. Wiborg, Department of Biostructural Chemistry, Aarhus University, for his generous gift of the plasmid pCP40.

* Supplementary material has been deposited with the IUCr (Reference: AD0015). Copies may be obtained through the Managing Editor, 5 Abbey Square, Chester CH1 2HU.

References

Bourne, H. R., Sanders, D. A. & McCormick, F. (1990). *Nature (London)*, **348**, 125–132.

Bourne, H. R., Sanders, D. A. & McCormick, F. (1991). *Nature (London)*, **349**, 117–127.

Brünger, A. T. (1992). *X-PLOR Version 3.1. A System for X-ray Crystallography and NMR*. Yale University Press, New Haven, CT, USA.

Esnouf, R., Ren, J., Ross, C., Jones, Y., Stammers, D. & Stuart, D. (1995). *Nature Struct. Biol.* **2**, 303–308.

Kawashima, T., Berthet-Colominas, C., Wulff, M., Cusack, S. & Leberman, R. (1996). *Nature (London)*. In the press.
Kraulis, P. J. (1991). *J. Appl. Cryst.* **24,** 946–950.
Leberman, R., Antonsson, B., Giovanelli, R., Guariguata, R., Schumann, R. & Wittinghofer, A. (1980). *Anal. Biochem.* **104,** 29–36.
Leberman, R., Schulz, G. E. & Suck, D. (1981). *FEBS Lett.* **124,** 279–281.
Navaza, J. (1994). *Acta. Cryst.* A**50,** 157–163.
Remaut, E., Tsao, H. & Fiers, W. (1983). *Gene*, **22,** 103–113.
Schick, B. & Jurnak, F. (1994). *Acta. Cryst.* D**50,** 563–568.
Schneider, U. (1983). Diplomarbeit Dissertation. Albert-Ludwigs-Universität, Freiburg im Breisgau, Germany.
Stammers, D. K., Somers, D. O'N., Ross, C. K., Kirby, I., Ray, P. H., Wilson, J. E., Norman, M., Ren, J. S., Esnouf, R. M., Garman, E. F., Jones, E. Y. & Stuart, D. I. (1994). *J. Mol. Biol.* **242,** 586–588.
Wittinghofer, A., Guariguata, R. & Leberman, R. (1983). *J. Bacteriol.* **153,** 1266–1271.
Wittinghofer, A. & Leberman, R. (1976). *Eur. J. Biochem.* **62,** 373–382.
Ziegler, A., Harrison, S. C. & Leberman, R. (1974). *Virology*, **59,** 505–515.